

Band offsets between amorphous LaAlO₃ and In_{0.53}Ga_{0.47}As

N. Goel,^{a)} W. Tsai, and C. M. Garner
Intel Corporation, Santa Clara, California 95052

Y. Sun and P. Pianetta
Stanford Synchrotron Radiation Laboratory, Stanford University, Stanford, California 94305-4075

M. Warusawithana and D. G. Schlom
Department of Materials Science and Engineering, Pennsylvania State University, University Park, Pennsylvania 16802-5005

H. Wen, C. Gaspe, J. C. Keay, and M. B. Santos
Homer L. Dodge Department of Physics and Astronomy, The University of Oklahoma, Norman, Oklahoma 73019

L. V. Goncharova, E. Garfunkel, and T. Gustafsson
Laboratory for Surface Modification, Rutgers University, 136 Frelinghuysen Rd., Piscataway, New Jersey 08854

(Received 15 July 2007; accepted 18 August 2007; published online 13 September 2007)

The band offsets between an amorphous LaAlO₃ dielectric prepared by molecular-beam deposition and a *n*-type In_{0.53}Ga_{0.47}As (001) layer have been measured using synchrotron radiation photoemission spectroscopy. The valence and conduction band offsets at the postdeposition annealed LaAlO₃/InGaAs interface are 3.1±0.1 and 2.35±0.2 eV, respectively. The band gap of LaAlO₃, as determined by Al 2*p* and O 1*s* core level energy loss spectra, is 6.2±0.1 eV. Within the resolution of the medium energy ion scattering technique, no interfacial oxide layer is seen between the InGaAs and the 3.6 nm thick amorphous LaAlO₃. © 2007 American Institute of Physics.
[DOI: 10.1063/1.2783264]

As we approach the fundamental limit to the scaling of the conventional complementary metal-oxide-semiconductor (MOS) transistors, high dielectric constant (high- κ) materials and high mobility, smaller band gap III-V channel materials¹ such as indium gallium arsenide (In_{*x*}Ga_{1-*x*}As) and indium antimonide are being actively investigated for future logic technology generations.^{2,3} To act as a barrier for both electron and hole injection, sufficient valence and conduction band discontinuities between the insulator and the semiconductor is desirable in such devices.^{4,5} Furthermore, to achieve less than 1 nm equivalent oxide thickness, an abrupt interface without an undesirable lower- κ interfacial layer is needed.

Due to several promising electrical and physical characteristics of molecular-beam deposited amorphous LaAlO₃ with Si,⁶⁻⁹ we have begun to explore the possibility of its inclusion as the gate dielectric in InGaAs-based devices. Minimal frequency dispersion, <40 mV hysteresis, and low leakage current density have been measured in LaAlO₃/In_{0.53}Ga_{0.47}As MOS capacitors.¹⁰ In addition, using high-resolution transmission electron microscopy and electron energy loss spectroscopy, the insulator layer was found to be amorphous and no undesirable oxide layer was observed at the LaAlO₃ and InGaAs interface despite annealing up to 500 °C.¹⁰ In this letter, we report the structural, chemical and electronic properties of thin amorphous LaAlO₃ on *n*-In_{0.53}Ga_{0.47}As as measured by medium-energy ion scattering (MEIS) and synchrotron radiation photoemission spectroscopy.

A 100 nm thick Si-doped In_{0.53}Ga_{0.47}As epilayer was deposited on a 100 nm thick *n*-type In_{0.52}Al_{0.48}As buffer layer grown on *n*⁺ InP (001) substrates in an Intevac GEN II molecular-beam epitaxy (MBE) system. The InGaAs samples were capped with an amorphous arsenic layer to minimize the interfacial defect density as well as native oxide formation during air transfer.¹¹ The arsenic cap was desorbed in an EPI 930 MBE in the absence of an arsenic overpressure. Amorphous LaAlO₃ was then deposited at 80 °C substrate temperature by a technique described previously.⁶⁻¹⁰

The electronic properties such as the valence band (ΔE_V) and conduction band offsets (ΔE_C) between LaAlO₃ and *n*-type InGaAs were then determined by photoemission spectra taken on beam lines 8-1 (photon energy range of 30–170 eV) and 10-1 (photon energy range of 200–1200 eV) at the Stanford Synchrotron Radiation Laboratory (SSRL). The Gaussian broadening by the analyzer and the beam line was about 0.15 eV. MEIS was performed, using an instrument described in detail elsewhere.^{12,13}

The MEIS spectrum of a 3.6 nm thick LaAlO₃ film on InGaAs (Fig. 1) has well separated oxygen, aluminum, gallium/arsenic, and lanthanum/indium peaks. The MEIS backscatter model analysis is consistent with an abrupt interface between the LaAlO₃ and InGaAs, assuming LaAlO₃ film stoichiometry of La:Al:O=1:1.1:3.1, within the 0.2–0.3 nm resolution of this analysis. Furthermore, nearly identical Al and O profiles (Fig. 1, inset) indicate the absence of any other oxygen-containing phase at the interface. Thus, no interfacial oxide layer is observed for the as-deposited LaAlO₃ (not shown) or after annealing at 440 °C (Fig. 1) or 500 °C (not shown).

^{a)} Author to whom correspondence should be addressed; FAX: 1-408-653-6790; electronic mail: niti.goel@intel.com

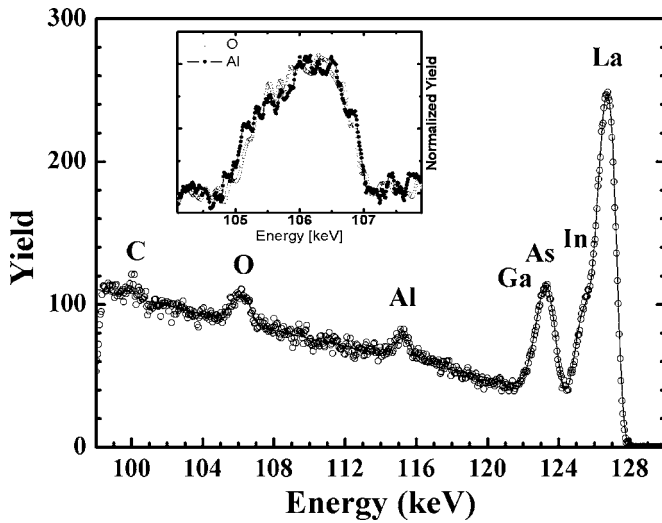


FIG. 1. MEIS energy spectrum (dots) of a 3.6 nm thick amorphous LaAlO_3 film on InGaAs after an *in situ* postannealing at 440 °C. The MEIS spectra were taken with a double channeling geometry in the InGaAs $[\bar{1}\bar{1}2]$ scattering plane, the incoming beam aligned with a $[100]$ channeling direction, and the detector axis aligned with an InGaAs $[111]$ axis. A H^+ beam with 130 keV energy and a scattering angle of 125.3° were typically used. The quantitative model data (line), where an oxide-free interface is assumed, is also shown. In the inset, the overlap of the Al peak with the O peak is shown (normalized, background subtracted).

The model proposed by Kraut *et al.*^{14,15} was used to determine ΔE_V .

$$\Delta E_V = (E_{\text{As } 3d} - E_V)_{\text{InGaAs}} - (E_{\text{Al } 2p} - E_V)_{\text{LaAlO}_3} - (E_{\text{As } 3d} - E_{\text{Al } 2p})_{\text{LaAlO}_3/\text{InGaAs}}, \quad (1)$$

where $E_{\text{As } 3d}$ and $E_{\text{Al } 2p}$ are the core level positions, E_V for InGaAs and LaAlO_3 are the valence band maximum (VBM) of these bulk materials, combined with the core level difference of the heterojunction ($\text{LaAlO}_3/\text{InGaAs}$). The $\text{LaAlO}_3/\text{InGaAs}$ samples were either as deposited or annealed at 440 or 500 °C in an UHV chamber to remove the adsorbed hydrocarbon and hydroxyls (OH) on the film surface.⁷ To remove the native oxide from InGaAs, the bulk sample was *ex situ* cleaned in dilute HF followed by annealing at 200 °C in UHV for a few minutes to eliminate the surface elemental arsenic (As–As) contribution to the reference As $3d$ peak.¹⁶ The As $3d$ signal of clean bulk InGaAs consists of a doublet with As $3d_{3/2}$ and $3d_{5/2}$ peaks where As $3d_{3/2}$ is at higher binding energy.

TABLE I. Summary of core levels, valence bands, conduction band offsets (ΔE_c), and valence band offsets (ΔE_V) for bulk *n*-type $\text{In}_{0.53}\text{Ga}_{0.47}\text{As}$, as-deposited and UHV-annealed amorphous LaAlO_3 films on *n*-type $\text{In}_{0.53}\text{Ga}_{0.47}\text{As}$.

Sample	UHV T_{anneal} (°C)	$E_{\text{As } 3d}$ (eV)	$E_{\text{Al } 2p}$ (eV)	E_{VBM} (eV)	ΔE_V (eV)	ΔE_c (eV)
Bulk clean InGaAs	200	40.8	...	0.37±0.05
15 nm $\text{LaAlO}_3/\text{InGaAs}$	Unannealed	...	75.15	4.36±0.05	3.12±0.1	2.33±0.2
	440	...	74.75	4.21±0.05	3.09±0.1	2.36±0.2
	500	...	74.7	4.19±0.05	3.12±0.1	2.33±0.2
1 nm $\text{LaAlO}_3/\text{InGaAs}$	Unannealed	41.04	74.52
	440	41.05	74.25
	500	40.95	74.15

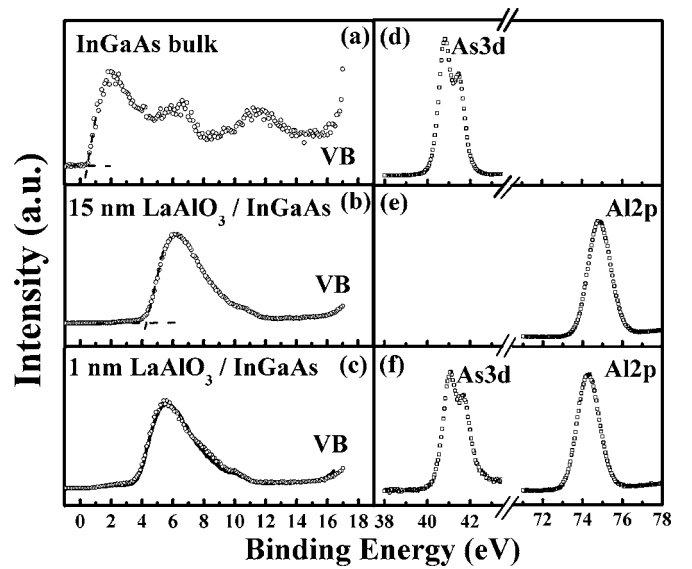


FIG. 2. Valence band and shallow core level synchrotron radiation photoelectron spectra for bare bulk *n*-type $\text{In}_{0.53}\text{GaAs}$ (001) [(a) and (d)], a 15 nm thick amorphous LaAlO_3 film [(b) and (e)], and a 1 nm thick $\text{LaAlO}_3/\text{InGaAs}$ heterojunction [(c) and (f)]. LaAlO_3 was *in situ* annealed at 440 °C. In (c), the simulated VB spectrum (solid line) is compared with the experimental VB spectra (open circles) of the as-grown $\text{LaAlO}_3/\text{InGaAs}$ heterojunction. The core levels and valence bands were measured with a photon energy source of 140 eV at normal incidence with the electron energy analyzer pass energy of 11.75 eV. For clarity, each spectrum is plotted with the maximum intensity scale for the respective peak.

The valence band (VB) spectra and core levels (Fig. 2) were used to establish the VB offsets. Using linear extrapolation method,¹⁷ the VBM energies for clean bulk InGaAs and a 15 nm thick amorphous LaAlO_3 were determined. The VBM and measured core level energies for annealed and as-deposited samples are summarized in Table I. The ΔE_V between LaAlO_3 and $\text{In}_{0.53}\text{Ga}_{0.47}\text{As}$ was then calculated using Eq. (1) (listed in Table I). Comparison of the LaAlO_3 (1 nm)/*n*-type InGaAs annealed interface spectra [Fig. 2(c), dots] with a simulated VB spectrum (line) suggests that there is negligible contribution of any interfacial layer. The simulated VB spectrum was produced by shifting and summing the VB data for the annealed 15 nm thick LaAlO_3 and clean bulk InGaAs.¹⁷ Similar data are seen for as-deposited and 500 °C annealed dielectric samples.

The band gap values of the dielectric were obtained from the photoemission spectra using the onsets of the electron energy loss signal for the Al $2p$ and O $1s$ core level peaks¹⁸

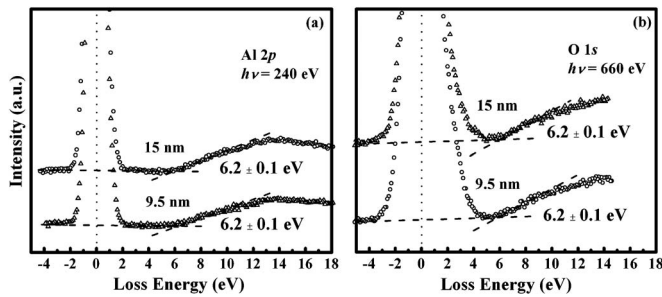


FIG. 3. Energy loss spectra of (a) Al 2p and (b) O 1s photoelectrons of 9.5 and 15 nm-thick amorphous LaAlO₃ films postdeposition annealed at 440 °C. The two curves in each plot are offset along the intensity axis for clarity. The band gap was determined by linear extrapolation, shown by the dashed lines.

by linearly extrapolating the segment of maximum negative slope to the background level, Fig. 3.¹⁶ The band gap of the as-deposited and annealed amorphous LaAlO₃ (E_g)_{LaAlO₃} was thus determined to be 6.2 ± 0.1 eV.

From the VBM and E_g values, the conduction band offset between LaAlO₃ and InGaAs given by

$$\Delta E_C = (E_g)_{\text{LaAlO}_3} - (E_g)_{\text{InGaAs}} - \Delta E_V \quad (2)$$

is calculated and listed in Table I. Here, $(E_g)_{\text{InGaAs}}$ is the band gap of In_{0.53}Ga_{0.47}As. We determined $\Delta E_V = 3.1 \pm 0.1$ eV and $\Delta E_C = 2.35 \pm 0.2$ eV for annealed LaAlO₃ on *n*-type In_{0.53}Ga_{0.47}As.

For comparison, reported experimental values of ΔE_V and ΔE_C between MBE LaAlO₃ and Si are 3.2 ± 0.1 and 1.8 ± 0.2 eV, respectively, for an amorphous LaAlO₃ film deposited by same technique.⁷ Using the charge neutrality level method, the calculated ΔE_C and ΔE_V of LaAlO₃ are 1.5 and 2.6 eV with GaAs and 2.5 and 2.7 eV with InAs, respectively.⁴ Considering that the band gap of crystalline LaAlO₃ (5.6 eV) used in these calculations¹⁹ is different than the band gap of our amorphous LaAlO₃ layer (6.2 eV), the experimental band offset values obtained here on In_{0.53}Ga_{0.47}As are close to a linear interpolation between these calculated band offsets.

In summary, we have used a combination of shallow core level and valence band photoemission measurements to directly determine the valence and conduction band offsets at the amorphous LaAlO₃/*n*-type In_{0.53}Ga_{0.47}As interface and the band gap of the dielectric. Within the resolution of MEIS,

no interfacial oxide layer was observed between InGaAs and a 3.6 nm thick LaAlO₃ overlayer.

Part of this study was carried out at SSRL, a national user facility operated by Stanford University on behalf of the U.S. Department of Energy, Office of Basic Energy Sciences. The authors are grateful to the SSRL staff for their support, Prof. M. Hong (NTHU) for discussion, and Intel for funding. MBS also acknowledges support from the NSF Grant No. DMR-0520550. L.V.G., E.G., and T.G. acknowledge the NSF and SRC for support.

¹R. Chau, S. Datta, and A. Majumdar, IEEE Compound Semiconductor Integrated Circuit Symposium, Technical Digest, 2005, pp. 17–20.

²D.-H. Kim, J. A. del Alamo, J. H. Lee, and K. S. Seo, Tech. Dig. - Int. Electron Devices Meet. **2005**, 767.

³S. Datta, T. Ashley, R. Chau, K. Hilton, R. Jefferies, T. Martin, and T. J. Phillips, Tech. Dig. - Int. Electron Devices Meet. **2005**, 783.

⁴J. Robertson, J. Vac. Sci. Technol. B **18**, 1785 (2000).

⁵P. W. Peacock and J. Robertson, J. Appl. Phys. **92**, 4712 (2002).

⁶E. Cicerrella, J. L. Freeouf, L. F. Edge, D. G. Schlom, T. Heeg, J. Schubert, and S. A. Chambers, J. Vac. Sci. Technol. A **23**, 1676 (2005).

⁷L. F. Edge, D. G. Schlom, S. A. Chambers, E. Cicerrella, J. L. Freeouf, B. Holländer, and J. Schubert, Appl. Phys. Lett. **84**, 726 (2004).

⁸P. Sivasubramani, M. J. Kim, B. E. Gnade, R. M. Wallace, L. F. Edge, D. G. Schlom, H. S. Craft, and J.-P. Maria, Appl. Phys. Lett. **86**, 201901 (2005).

⁹L. F. Edge, D. G. Schlom, R. T. Brewer, Y. J. Chabal, J. R. Williams, S. A. Chambers, C. Hinkle, G. Lucovsky, Y. Yang, S. Stemmer, M. Copel, B. Holländer, and J. Schubert, Appl. Phys. Lett. **84**, 4629 (2004).

¹⁰N. Goel, P. Majhi, W. Tsai, M. Warusawithana, D. G. Schlom, M. B. Santos, J. S. Harris, and Y. Nishi Appl. Phys. Lett. **91**, 093509 (2007).

¹¹S. P. Kowalczyk, D. L. Miller, J. R. Waldrop, P. G. Newman, and R. W. Grant, J. Vac. Sci. Technol. **19**, 255 (1981).

¹²W. H. Schulte, B. W. Busch, E. Garfunkel, T. Gustafsson, and G. Schiwietz, Nucl. Instrum. Methods Phys. Res. B **183**, 16 (2001).

¹³R. M. Tromp, M. Copel, M. C. Reuter, M. Horn von Hoegen, and J. Speidell, Rev. Sci. Instrum. **62**, 2679 (1991).

¹⁴E. A. Kraut, R. W. Grant, J. R. Waldrop, and S. P. Kowalczyk, Phys. Rev. Lett. **44**, 1620 (1980).

¹⁵E. A. Kraut, R. W. Grant, J. R. Waldrop, and S. P. Kowalczyk, Phys. Rev. B **28**, 1965 (1983).

¹⁶Z. Liu, Y. Sun, F. Machuca, P. Pianetta, W. E. Spicer, and R. F. W. Pease, J. Vac. Sci. Technol. B **21**, 1953 (2003).

¹⁷S. A. Chambers, Y. Liang, Z. Yu, R. Droopad, J. Ramdani, and K. Eisenbeiser, Appl. Phys. Lett. **77**, 1662 (2000); S. A. Chambers, Y. Liang, Z. Yu, R. Droopad, and J. Ramdani, J. Vac. Sci. Technol. A **19**, 934 (2001).

¹⁸S. Miyazaki, J. Vac. Sci. Technol. B **19**, 2212 (2001); S. A. Chambers, T. Droubay, T. C. Kaspar, and M. Gutowski, *ibid.* **22**, 2205 (2004).

¹⁹S.-G. Lim, S. Kriventsov, T. N. Jackson, J. H. Haeni, D. G. Schlom, A. M. Balbashov, R. Uecker, P. Reiche, J. L. Freeouf, and G. Lucovsky, J. Appl. Phys. **91**, 4500 (2002).